

Cold-formed steel channel beams: From optimal design to development of a novel section

Jun Ye, Iman Hajirasouliha, Jurgen Becque

University of Sheffield

jye2@sheffield.ac.uk, i.hajirasouliha@sheffield.ac.uk, j.becque@sheffield.ac.uk

Primary Supervisor: Dr I. Hajirasouliha – e-mail: i.hajirasouliha@sheffield.ac.uk
Secondary Supervisor: Dr J. Becque – e-mail: j.becque@sheffield.ac.uk

ABSTRACT. Optimal design of cold-formed steel (CFS) cross-sections can significantly increase their ultimate load carrying capacity leading to a more economical and efficient structural system. This paper reports on the result of an investigation on optimisation of CFS channel beams subjected to their bending capacity. The optimisation was aimed at maximize strength complying with the manufacturing and constructional restraints. As a result, the selected prototypes and optimisation process met the requirements suggested in Eurocode 3 (EC3). In total, ten CFS channel cross-sections including one novel channel section with the folded flange were considered in the optimisation process. The cross-sectional properties and flexural strength of the sections were determined based on the effective width method suggested in EC3, while the optimisation process was performed using particle swarm optimisation method. The flexural strength of the optimised sections were also obtained using the nonlinear finite element (FE) analysis and the results were compared with those of effective width method suggested in EC3. For the newly-developed folded-flange section, it was observed that the suggested model can predict the bending capacity with reliable accuracy. In addition, compared to their commonly-used standard counterpart and other optimised cross-sections with the same material, this new prototype possesses the highest bending capacity. The bending capacity can also be significantly enhanced by adding edge stiffeners while the effect of incorporating the intermediate stiffeners is negligible and even negative in some cases.

KEYWORDS. Optimisation; Cold-formed steel beams; Folded flange section; Effective width method; Finite element analysis.

INTRODUCTION

The flexibility of profile shapes allows more choices for designers. However, CFS members are inherently vulnerable to the multitude buckling behaviours which make the design procedure complex and time-consuming. Recent experimental and analytical research [1] has demonstrated that increasing the number of flange bends in CFS channel sections can enhance both the elastic and inelastic behavior. Consequently, the highest strength, stiffness, and ductility were observed in beams with an infinite number of bends (curved flanges) as shown in Fig. 1(a). Nevertheless, this type of cross-section is hard to manufacture and difficult to connect with floor systems. By considering the construction and manufacture restraints, the curved flange can be substituted with a folded flange as shown in Fig. 1(b). This folded flange section along with nine other conventional channel sections were considered as the prototypes in the current study. A constant total coil width and thickness were considered for all section during the optimisation process. The flexural properties of the sections were determined in accordance to the Effective Width Method suggested in EC3 [2]. The optimised solutions were arrived using Particle Swarm Optimisation (PSO) Algorithm [3].

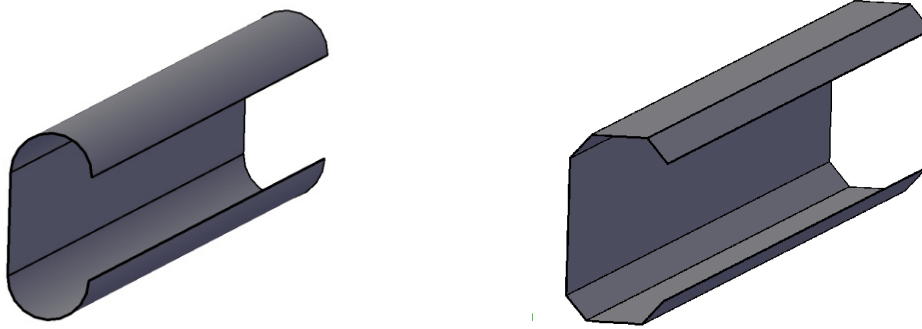


Figure 1. CFS channel sections with curved flange and folded flange.

DESIGN OF CFS MEMBERS BASED ON EC3

The optimal design of the selected prototypes followed the stability and strength provisions suggested based on the Effective Width Method in EC3. EC3 uses the notional flat width of the plate assemblies to determine the cross-sectional properties and these properties are reduced by a factor (δ) to account for the round corner effects.

Design for local buckling

In EC3, the effect of local buckling is considered through the effective width concept, first proposed by Von Karman [4]. It recognizes the fact that local buckling of the plates constituting the cross-section has the effect of shifting the load-bearing stresses towards the corner zones, while the central parts of the plates become less effective in carrying load. This effective area is assumed to carry the full compressive load applied to the section. According to EC3, the effective width of a plate is given by

$$\frac{b_e}{b} = \frac{1}{\lambda_l} \left(1 - \frac{0.055(3+\psi)}{\lambda_l} \right) \quad (1)$$

where b and b_e are the total and the effective width of the plate, respectively. Also, the slenderness against local buckling, $\lambda_l = \sqrt{f_y / \sigma_{cr}}$, relates to the material yield stress, f_y , and the elastic local buckling stress of the plate, σ_{cr} . ψ is the stress ratio of the plates.

Design for Distortional buckling

In EC3, the design of distortional buckling is based on the assumption that the stiffeners of compressive flange behave as a strut with springs along the centroid axis. The elastic critical buckling stress for stiffened elements is then defined by

$$\sigma_{cr,s} = \frac{2\sqrt{KEI_s}}{A_s} \quad (2)$$

where $\sigma_{cr,s}$ is the elastic critical buckling stress, E is the modulus of elasticity, I_s is the second moment of the effective area of the stiffener about the axis parallel to flange, K is the spring stiffness per unit length, and A_s is the effective area of the edge stiffener. For the folded flange cross-section, two distortional buckling modes are probable depending on the length of flange parts. As demonstrated Figs. 2(a) and 2(b), where the length of flange 2 is relatively larger than flange 1, buckling of sub-assembly of flange 2 and lip may occur, while the second buckling modes will be expected when flange 1 is much longer than flange 2. The deflections δ_1 and δ_2 produced by concentrated forces u_1 and u_2 , respectively, are defined by

$$\delta_1 = \frac{u_1}{3D} \left[e^3 + e^2b + b(e - b\cos\theta_1)(2e - b\cos\theta_1) + \frac{3}{2}b(e - b\cos\theta_1)^2 \right] \quad (3)$$

$$\delta_2 = \frac{u_2}{3D} \left[e^3 + \frac{3}{2} b e^2 \right] \quad (4)$$

where the bending rigidity of the plate $D = Et^3 / 12(1 - \nu^2)$, e is the distance between the gravity centre of the edge stiffener to the web-to-flange junction, b is the height of web, b is the length of flange 1 and θ_1 is the angle between flange 1 and flange 2, as shown in Figs. 2, t is the thickness, E and ν are the modulus of elasticity and Poisson's ratio, respectively. The distortional buckling is taken into account by using a reduced thickness at the stiffeners.

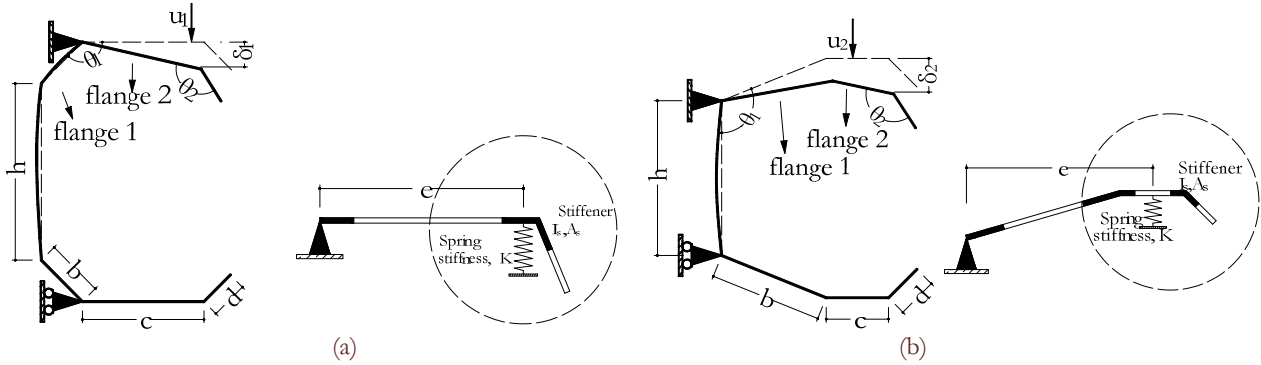


Figure. 2: Analytical model (a) to analyse distortional buckling-type 1 and (b) to analyse distortional buckling-type 2.

OPTIMISATION PROCEDURE

Problem definition

The optimisation procedure was aimed at optimising the each CFS cross-section with regard to its bending capacity. In order to take the manufacturing and construction issues into consideration, the optimal design formulation of CFS beams was derived based on the provisions suggested in EC3. In total, 10 different prototypes, including 9 prototypes predefined by EC3 and the newly-developed folded flange channel section were considered with the same thickness of $t = 1.5 \text{ mm}$ and total coil width of $l = 415 \text{ mm}$. Since the beams are always laterally supported by the floor system, only local/distortional buckling are considered in the optimisation process. Tab. 1 shows the selected prototypes along with the design variables and optimisation constraints. The yield strength of the CFS plate was considered to be $f_y = 450 \text{ MPa}$.

In the optimisation process, the length of intermediate stiffeners is 10 mm and the angle between the intermediate stiffeners is set to be 60° . The optimisation problem can be formulated as a minimization problem defined by

$$\min f(x) = -W_{eff} f_y / \gamma_{M_0} \quad u_{\min} \leq x_i \leq u_{\max} \quad \text{for } i = 1, \dots, N \quad (6)$$

where $f(x)$ is the design moment resistance of a cross-section about the major axis and W_{eff} is the effective section modulus which can be calculated based on the effective width of plates and the reduced thickness for distortional buckling. Also, γ_{M_0} is the partial factor of ultimate limit state. It is worth mentioning that the inelastic reserve capacity is always taken into account according to EC3. For each variable x_i , the lower and upper bounds, u_{\min} and u_{\max} , respectively, are considered according to EC3 and summarised in Tab. 2.

Optimisation solutions

The optimisation procedures were formulated in Matlab software [5] using the Particle Swarm Optimisation Algorithm. The population of particle swam was taken as 100, and the same number was also used for iterations to obtain the optimum value. For optimisation, each of the prototypes was run for 3 times and the result with maximum bending capacity was chosen as the optimum section. Tab. 2 summarise the geometrical details and bending capacity of the optimised cross-sections and Tab. 3 listed all the effective cross-sections of the optimised prototypes from Matlab which are drawn at the same scale.



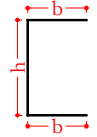
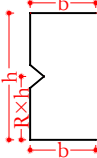
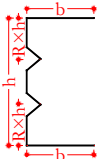
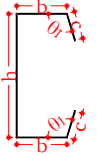
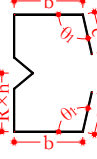

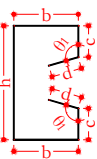
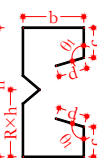
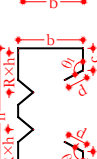
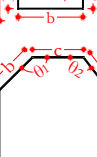
Prototype	Prototype section	Design variables	Constraints based on EC3	Comments
①		$x=b/l$	$b/t \leq 50$ $h/t \leq 500$	EN1993-1-3 Clause 5.2
②		$x_1=b/l$ $x_2=R$	$b/t \leq 50$ $h/t \leq 500$ $0.1 \leq R \leq 0.9$	EN1993-1-3 Clause 5.2
③		$x_1=b/l$ $x_2=R$	$b/t \leq 50$ $h/t \leq 500$ $0.1 \leq R \leq 0.9$	EN1993-1-3 Clause 5.2
④		$x_1=c/b$ $x_2=b/l$ $x_3=\theta_1$	$0.2 \leq c/b \leq 0.6$ $b/t \leq 60$ $c/t \leq 50$ $h/t \leq 500$ $\pi/4 \leq \theta_1 \leq 3/4\pi$	EN1993-1-3 Clause 5.2
⑤		$x_1=c/b$ $x_2=b/l$ $x_3=R$ $x_4=\theta_1$	$0.2 \leq c/b \leq 0.6$ $b/t \leq 60$ $c/t \leq 50$ $h/t \leq 500$ $\pi/4 \leq \theta_1 \leq 3/4\pi$ $0.1 \leq R \leq 0.9$	EN1993-1-3 Clause 5.2
⑥		$x_1=c/b$ $x_2=b/l$ $x_3=R$ $x_4=\theta_1$	$0.2 \leq c/b \leq 0.6$ $b/t \leq 60$ $c/t \leq 50$ $h/t \leq 500$ $\pi/4 \leq \theta_1 \leq 3/4\pi$ $0.1 \leq R \leq 0.4$	EN1993-1-3 Clause 5.2
⑦		$x_1=c/b$ $x_2=d/b$ $x_3=b/l$ $x_4=\theta_1$	$0.2 \leq c/b \leq 0.6$ $0.1 \leq d/b \leq 0.3$ $b/t \leq 90$ $c/t \leq 60$ $d/t \leq 50$ $h/t \leq 500$ $\pi/4 \leq \theta_1 \leq 3/4\pi$	EN1993-1-3 Clause 5.2
⑧		$x_1=c/b$ $x_2=d/b$ $x_3=b/l$ $x_4=R$ $x_5=\theta_1$	$0.2 \leq c/b \leq 0.6$ $0.1 \leq d/b \leq 0.3$ $b/t \leq 90$ $c/t \leq 60$ $d/t \leq 50$ $h/t \leq 500$ $\pi/4 \leq \theta_1 \leq 3/4\pi$ $0.1 \leq R \leq 0.9$	EN1993-1-3 Clause 5.2
⑨		$x_1=c/b$ $x_2=d/b$ $x_3=b/l$ $x_4=R$ $x_5=\theta_1$	$0.2 \leq c/b \leq 0.6$ $0.1 \leq d/b \leq 0.3$ $b/t \leq 90$ $c/t \leq 60$ $d/t \leq 50$ $h/t \leq 500$ $\pi/4 \leq \theta_1 \leq 3/4\pi$ $0.1 \leq R \leq 0.4$	EN1993-1-3 Clause 5.2
⑩		$x_1=\theta_1$ $x_2=\theta_2$ $x_3=b$ $x_4=c$ $x_5=d$	$h/t \leq 500$ $7/12\pi \leq \theta_1 \leq 5/6\pi$ $\pi/4 \leq \theta_2 \leq 3/4\pi$ $30 \leq b \leq 48$ $50 \leq c \leq 60$ $15 \leq d \leq 60$	Newly developed shape

Table 1: Selected prototypes, design variables and constraints.

It is clearly from Tab. 3 that all the cross-sections have the high height-to-width ratio. While the bending moments of the cross-sections are mainly determined by the effective portions of the plate assemblies and the web height, prototype 1-3 are still with low relatively bending strength though they have the biggest height. This is due to the fact that the flanges without edge stiffeners are susceptible to local buckling though the strength is slightly enhanced by adding intermediate stiffeners to the web. Comparing prototype 4 with prototypes 5 and 6 in Tab. 2 and 3 indicates that the introduction of edge stiffeners can significantly improve the bending capacities while it is not significant for the case of intermediate stiffeners. This is due to the fact: 1. the stiffeners are prone to distortional buckling with the high web dimension, leading to the loss of thickness of the intermediate stiffeners (as shown in Tab. 2), and 2. The folding of the intermediate stiffeners causes reduction of the height which is important to the effective sectional modulus.

Section	h (mm)	b (mm)	c (mm)	d (mm)	θ_1 (rad)	θ_2 (rad)	R	Capacity (kN·m)
①	315	50	-	-	-	-	-	9.84
②	305	50	-	-	-	-	0.856	11.08
③	295	50	-	-	-	-	0.186	9.92
④	269.8	50	22.6	-	1.579	-	-	13.38
⑤	263	50	21	-	1.61	-	0.79	13.66
⑥	234.4	50	20.3	-	1.576	-	0.223	12.69
⑦	242	50	29.3	7.2	1.574	-	-	15.11
⑧	240.6	50	25.3	6.9	2.356	-	0.9	14.62
⑨	231.8	50	25.2	6.4	2.356	-	0.1	13.41
⑩	184.6	48	50	17.2	1.83	1.66	-	16.12

Table 2: Geometrical details and bending capacities of the optimised sections.

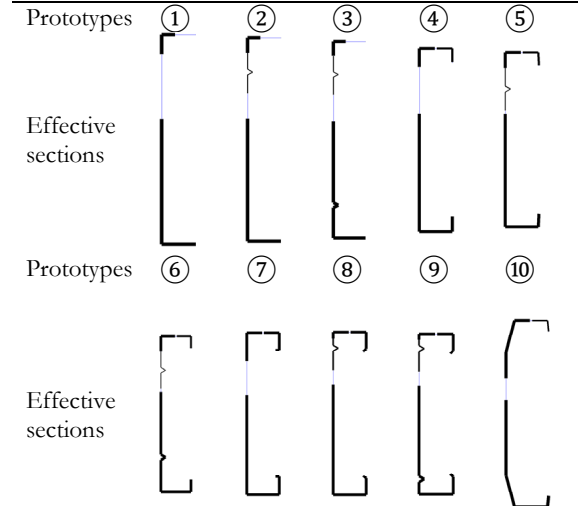


Table 3: Effective cross-sections of the beams.

Section	FE length (mm)	Bending moment (kN·m)		EC3/FE
		EC3	FEM	
Standard	1800	10.3	10.4	0.99
①	600	9.84	9.11	1.08
②	600	11.08	11.22	0.99
③	600	9.92	9.41	1.05
④	1800	13.38	12.73	1.05
⑤	1800	13.66	12.08	1.13
⑥	1800	12.69	11.15	1.14
⑦	2400	15.11	14.09	1.07
⑧	2400	14.62	12.99	1.13
⑨	2400	13.41	12.33	1.09
⑩	2400	16.12	15.52	1.04

Table 4: Comparison of the bending moment capacities of the optimised and standard sections obtained from EC3

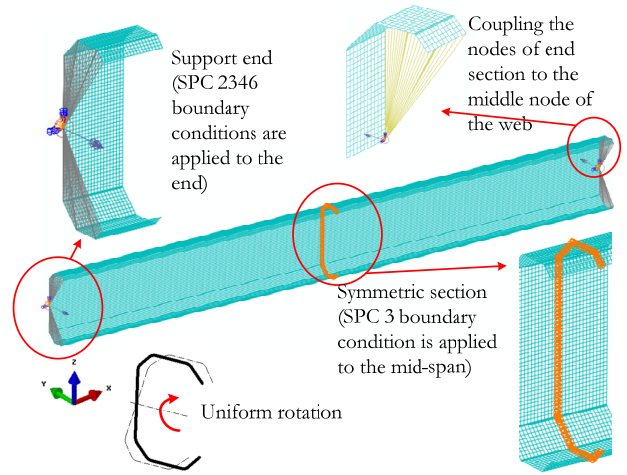


Figure 3: FE analysis and FE models of the beams subjected to local/distortional buckling.

NONLINEAR FE RESULTS OF THE STANDARD AND OPTIMISED CROSS-SECTIONS

The bending moment capacities of the optimised and standard cross-sections were also obtained using the nonlinear FE analysis with ABAQUS [6] and the results were compared with those determined according to the effective width method suggested in EC3. The adopted boundary conditions, material properties and imperfections were the same as the FE models in reference [7-9], accordingly and the load was applied in the form of



uniform rotations at both ends with a displacement control regime, as shown in Fig. 3. Also, the length of the beam models were selected as three times of distortional buckling half-wave length, as shown in Tab. 4. The FE modelling has been verified through the experimental results from [10, 11], good agreement has been achieved where the average error is around 10%.

Tab. 4 compares the bending capacities of the optimal and standard cross-sections obtained from the FE analysis with those determined based on the effective width method suggested in EC3. Despite that the results obtained from EC3 are unconservative compared to the FE bending capacities, it can be concluded that the Effective Width Method suggested in EC3 provides a reasonable prediction for bending moment capacities.

COMPARISON OF THE RESULTS AND DISCUSSION

Fig. 4 compares the bending moment capacities of optimised sections with that of the standard section. As observed in the prototypes, the following conclusions can be drawn:

- The newly-developed folded-flange section offers the highest bending moment capacity with 57% increase compared to the standard section.
- Adding edge stiffeners can result in a significant increase in the bending moment capacity of the section with a fix total coil width. This can be due to the effect of the edge stiffeners in preventing the distortional failure modes by increasing the elastic critical stress and the less reduction of the thickness.

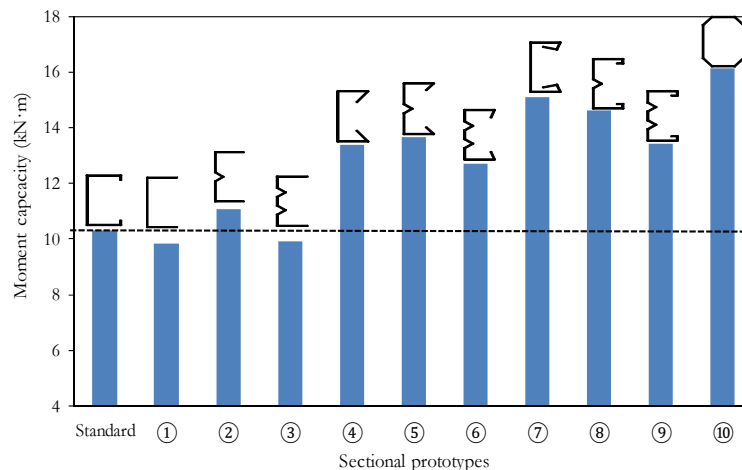


Figure 4: Comparison of the moment capacity of prototypes

- Providing intermediate stiffeners in the web cannot essentially increase the optimal bending capacity. Although, intermediate stiffeners can significantly increase the effective width of the web, it reduces the total height of the cross-section with constant coil length which may cause a decrease in the effective sectional modulus.
- The plain channel cross-sections cannot be considered as effective and economical cross-section in term of bending capacity.

REFERENCES

- [1] Sabbagh, A.B., Petkovski, M., Pilakoutas K., Mirghaderi R., Ductile moment-resisting frames using cold-formed steel sections: An analytical investigation. *J. Constr. Steel. Res.*, 67(2011) 634-646.
- [2] Eurocode 3: design of steel structures: Part 1.1: General rules and rules for buildings. EN 1993-1-1; (2005).
- [3] Perez, R.E., Behdinan, K., Particle swarm approach for structural design optimisation. *Comput Struct.*, 85(2007)1579-1688.
- [4] Von Karman, T., Sechler, E.E., Donnell, L., The strength of thin plates in compression. *Trans ASME.*, 54(1932) 53-57.
- [5] Mathworks. Matlab R2011a. Mathworks, Inc; (2011).
- [6] ABAQUS. Version 6.7 ed. Pawtucket, USA: Hibbitt, Karlsson & Sorensen, Inc; (2007).

- [7] Shifferaw, Y., Schafer, B.W., Inelastic Bending Capacity of Cold-Formed Steel Members. *J Struct Eng-ASCE.*, 138 (2012) 468-480.
- [8] Haidarali, M.R., Nethercot, D.A., Finite element modelling of cold-formed steel beams under local buckling or combined local/distortional buckling. *Thin Wall Struct.*, 49 (2011) 1554-62.
- [9] Schafer, B.W., Pekoz, T., Computational modeling of cold-formed steel: characterizing geometric imperfections and residual stresses, *J Constr Steel Res.*, 47 (1998) 193-210.
- [10] Yu, C., Schafer, B.W., Distortional buckling tests on cold-formed steel beams. *J Struct Eng-ASCE*, 132 (2006) 515-528.
- [11] Yu, C., Schafer, B.W., Local buckling tests on cold-formed steel beams, *J Struct Eng-ASCE.*, 129 (2003) 1596-1606.